Development of an Efficient Transdermal Delivery System of Small Interfering RNA Using Functional Peptides, Tat and AT-1002

Tamae Uchida,[#] Takanori Kanazawa,[#] Yuuki Takashima, and Hiroaki Okada*

Laboratory of Pharmaceutics and Drug Delivery, Department of Pharmaceutical Science, School of Pharmacy, Tokyo University of Pharmacy and Life Sciences; 1432–1 Horinouchi, Hachioji, Tokyo 192–0392, Japan.
Received August 24, 2010; accepted November 10, 2010; published online November 24, 2010

Topical use of small interfering RNA (siRNA) as a therapeutic nucleic acid is increasingly studied for the treatment of skin diseases and for the improvement of skin properties. However, naked siRNA transdermal delivery is limited by its low stability in the body and low permeability into target cells. This is due to various skin barriers such as the stratum corneum that has multiple lipid bilayers and epidermal layers that have tight junctions. In this study, we investigate non-invasive transdermal siRNA delivery using two functional peptides: AT1002, which is a tight junction modulator and 6-mer synthetic peptide belonging to a novel class of compounds that reversibly increases paracellular transport of molecules across the epithelial barrier; and Tat, which is a cell-penetrating peptide applicable as a transdermal siRNA delivery enhancer. We examined whether expression of the tight junction protein zonula occludens protein 1 (ZO-1) was detected in mouse skin applied with AT1002. Additionally, siRNA stabilities for RNaseA using Tat and AT1002 were assessed. We also determined the intradermal delivery efficiency of siRNA using functional peptides by confocal laser microscopy of fluorescently labeled siRNA in mouse skin. We found that the Tat analog and AT1002 strongly increased siRNA stability against RNaseA. In addition, ZO-1 disappeared from the skin after treatment with AT1002, yet recovered with time after washing. Finally, we also found that Tat and AT1002 peptides accelerate transdermal siRNA delivery both widely and effectively. Thus, combination of Tat and AT1002 is expected to be a transdermal delivery enhancer of siRNA.

Key words transdermal small interfering RNA delivery; cell penetrating peptide; AT1002; tight junction modulator; zonula occludens protein 1

Topical use of therapeutic peptides, proteins and nucleic acids, such as plasmid DNA and small interfering RNA (siRNA), has been increasingly studied due to the importance of treating skin diseases, topical vaccination, and improving skin properties.[1,2] In particular, siRNA has been investigated as a novel drug for allergic skin diseases due to its target-factor silencing effect. However, topical application of naked siRNA does not exert strong therapeutic effects due to its low delivery efficiency to target tissues and cells by various skin barriers like stratum corneum (SC) and epidermis, and due to its degradation by enzymes in the body.

The most important function of skin is to form an effective barrier between the internal and external layers of the organism, primarily the epidermis, which mostly comprises the physical barriers. Although the SC is recognized as an important physical barrier, nucleated epidermal layers are also significant for barrier function and so too are tight junctions (TJ).[3] TJ are cell–cell junctions that connect each neighboring cell and control the paracellular pathway of molecules. In human epidermis, various TJ proteins including occludin, claudin, and zonula occludens protein 1 (ZO-1) have been identified.[4,5] In addition, TJ proteins also appear to play a role in basic barrier function of biological membranes, as suggested by the phenotype of several mouse models.[6]

On skin diseases, such as atopic dermatitis where the SC is disrupted, the transport of molecules through the SC is considered to not be that difficult. However, in the epidermis, the granular layer has low permeation due to the barriers that are formed by tight junctions. Even though paracellular delivery to the epidermal layer in atopic dermatitis skin is considered a good method, it seems to be very difficult to achieve. As a result, physical enhancement methods, for example, iontophoresis, sonophoresis and electroporation, have been developed to improve transdermal delivery. However, these methods are considered difficult to use because of their invasive topical damage and so less-invasive and easier topical delivery methods should be considered.

In the case of mucosal application of drugs, several tight junction modulators, such as chitosans[7—9] and the cloudin-4 modulator[10—12] have been used as absorption enhancers. Furthermore, Zonula occludens toxin (Zot) has been shown to reversibly open the tight junction between cells and thereby increase the paracellular transport of several drugs in a non-toxic manner.[13—15] Zot is a 45-kDa protein located in the cell envelope of *Vibrio cholerae*. As an alternative to Zot, advances in the study of structure–activity relationships have led to the identification of AT1002, a novel tight junction modulator peptide.[16,17] AT1002 is a six-mer synthetic peptide that retains non-toxic biological activity by reversibly opening tight junctions, like Zot, and increases paracellular transport of drugs across the epithelial barrier.

Several proteins with basic protein transduction domains (PTDs), also called cell-penetrating peptides (CPP) or membrane transduction peptides, have been identified and are capable of passing through the plasma membrane of cells of animals[18] and plants.[19] Moreover, peptides with PTDs can deliver biologically active cargoes across membrane barriers and into the cell.[20] A list of transducible PTD-fusion proteins has been published.[21] Different PTD-cargo conjugates can be targeted either to the cytoplasm, organelle or nucleus in a variety of animal cell lines.[22—24] The ability of PTDs to penetrate the skin of living animals was first demonstrated by a study using a conjugated hepta-arginine peptide.[25] Subsequently, several PTDs have also been reported to carry conju-

* To whom correspondence should be addressed. e-mail: okada@toyaku.ac.jp
[#] These authors contributed equally to this work.

Table 1. Sequences of siRNAs

		Sequence	M.W.
FAM-labeled siRNA (FAMsiRNA)	Sense	5′ AUC CGC GCG AUA GUA CGU ATT 3′	13315.2
	Antisense	5′ 6-FAM UAC GUA CUA UCG CGC GGA UTT 3′	
siRNA for GL3 (siGL3)	Sense	5′ GGU GCA GAA AGA AGA CAU UTT 3′	13285
	Antisense	5′ AAU GUC UUC UUU CUG CAC CTT 3′	
siRNA for RelA (siRelA)	Sense	5′ GGU GCA GAA AGA AGA CAU UTT 3′	13285
	Antisense	5′ AAU GUC UUC UUU CUG CAC CTT 3′	

gated compounds into animal skin.[26,27] Additionally, we previously reported that CPP (Tat peptide) could improve topical gene expression in the mouse vagina when transfected to mice vaginally.[28]

In this study, we investigated whether modulators of TJs and CPPs could be applicable to the non-invasive and effective transdermal siRNA delivery system for treating skin diseases. We synthesized the AT1002 and Tat analogs as enhancers for transdermal siRNA delivery. In order to determine the potency of the TJ modulator AT1002 applied to mouse skin, the expression of ZO-1, one of the tight junction factors, was examined. We also assessed the stability of the siRNAs against RNaseA when in complex with Tat and/or AT1002. Furthermore, tape-stripping methods to disrupt the SC and the construction of an atopic dermatitis (AD)-like skin model were developed to observe the translocation of fluorescence-labeled siRNA with Tat and AT1002 in the mouse skin by confocal laser microscopy.

Experimental

siRNAs The siRNA oligonucleotides for luciferase (siGL3) and mouse RelA (siRelA) were designed and synthesized by NIPPON GENE Co., Ltd. (Tokyo, Japan), and 6-carboxyfluorescein (6-FAM)-labeled non-silencing siRNA (FAMsiRNA) was obtained from B-Brige Co. (Tokyo, Japan). The sequences of the sense and antisense oligos are shown in Table 1. Each siRNA was diluted to a final concentration of 1 mg/ml.

Animals Female 6-week-old ICR mice were purchased from SLC (Hamamatsu, Japan). The mice were housed under standard conditions of temperature (22—24 °C), humidity (40—60%) and 12-h-light/dark-cycles with the light period starting at 08:00 h. Food and water were supplied *ad libitum*. The Animal Care and Ethics Committee of Tokyo University of Pharmacy and Life Sciences (TUPLS) approved all of the experiments.

Peptides The Tat analog, which has Cys-Gly-NH_2 added to the N terminus of human immunodeficiency virus (HIV)-Tat (48—57), and the AT1002 analog, which has Gly and Cys-Gly-NH_2 added to the C and N termini of AT1002 (Table 2), were synthesized using the Fmoc-solid-phase peptide synthesis method with an ABI 433A peptide synthesizer (Applied Biosystems, Japan), as previously reported.[28,29] Both analogs were used after purification by reverse-phase HPLC. The molecular weight of each analog was determined by matrix-assisted laser desorption ionization time-of-flight mass spectrometry (MALDI-TOF-MS): Tat analog, 1627; AT1002 analog, 939.

Preparation of siRNA Complexes Tat and siRNA complexes (Tat) at the N/P ratio 1, 10 were prepared by incubating the peptides for 30 min at 4 °C. The AT1002 and siRNA mixing solution (AT1002) was prepared by mixing the two components at a molecular weight ratio of 80 for 30 min at 4 °C. The Tat/siRNA complex and AT1002 mixing solution (Tat+AT1002) were prepared by incubating the Tat/siRNA complex and AT1002 for 30 min at 4 °C.

Characterization of Tat/siRNA The mean diameter and size distribution of the Tat/FAMsiRNA complexes were measured using a DLS-700 unit (Otsuka Electronics Co., Ltd., Osaka, Japan). Zeta potential was measured using a NICOMP 380ZLS unit (Particle Sizing Systems, Shanghai, China).

siRNA Stability against RNaseA RNaseA (10 ng) was added to naked siRelA (Naked), the Tat/siRelA complex (Tat), the siRelA and AT1002 mixing solution (AT1002), and to the Tat/siRelA complex and AT1002 mixing solution (Tat+AT1002), and incubated at 37 °C for 10 h. The siRelA was decondensed from siRelA complexes by adding 0.01 mM dextran sulfate and the siRelA was labeled with SYBER® Green. Relative amounts of remaining siRelA were determined using a microplate reader. The data are expressed as relative remaining siRelA ratio *versus* the value of siRelA fluorescence at 0 h.

Table 2. Sequences of Tat and AT1002 Analogs

Name	Sequence
AT1002 analog (AT1002)	Phe-Cys-Ile-Gly-Arg-Leu-Cys-Gly
Tat analog (Tat)	Gly-Arg-Lys-Lys-Arg-Arg-Gln-Arg-Arg-Arg-Cys-Gly

***In Vitro* Study** PAM212 cells (keratinocytes) were cultured to 70—80% confluence in Dulbecco's Modified Eagle's Medium (DMEM) (Invitrogen Co., U.S.A.) supplemented with 10% fetal bovine serum (FBS) (Invitrogen Co., U.S.A.) and 1% penicillin/streptomycin (stock 10000 U/ml, 10000 mg/ml, Invitrogen Co., U.S.A.). PAM212 cells seeded onto 24-well plates at a density of 1×10^5 cells/well with 1 ml of FBS(+)DMEM were incubated at 37 °C in a humidified 5% CO_2 atmosphere for 24 h before the transfection study. After 24 h incubation, the cells were rinsed and 1 ml of DMEM without FBS was added to each well. Either naked siRelA (Naked) or Tat/siRelA complex (Tat) solution (100 μl containing siRelA: 0.05 mg) was applied to each well. After 24 h, cells were washed twice with phosphate buffered saline (PBS) and total RNA was isolated using TRIzol reagent (Invitrogen) according to the manufacturer's instructions. The primers were designed for polymerase chain reaction (PCR) amplification of cDNA and for the quantification of RelA by real-time PCR. cDNA was synthesized using total RNA and PrimeScript™ reagent kit (Takara, Japan) at 42 °C for 15 min and then 85 °C for 5 s. Real-time PCR was performed with cDNA, TaqMan® universal PCR master Mix, No AmpErase® UNG (Applied Biosystems, U.S.A.), and Primers. The expression level of glyceraldehyde-3-phosphate dehydrogenase (GAPDH) was determined as the internal control. The PCR primers to detect mouse GAPDH were from TaqMan®Gene Expression Assays (product code; Mm99999915_g1). To detect mouse RelA (Forward 5′-gtgcgacaaggtgcagaaag-3′; Reverse 5′-ccgatgcacatcagcttgag-3′) the primers were designed by NIPPON EGT Co., Ltd. (Toyama, Japan). According to the cycle threshold (Ct) value and standard curve equation, the relative content of mRNA was calculated and normalized as the mRNA expression of RelA in each sample. The data are expressed as the relative RelA mRNA ratio *versus* the control value.

Fluorescent Labeling The siGL3 was labeled using the Label IT nucleic acid labeling kit (Mirus Bio LLC, Milwaukee, WI, U.S.A.). Following a protocol provided by the manufacturer, 50 μl of siGL3 solution (1 mg/ml) and the same amount of Label IT reagent (Cy3) were mixed in 20 mM 3-(*N*-morpholino)propanesulfonic acid buffer (pH 7.5) and incubated at 37 °C for 2 h. Any of the labeling reagent that had not reacted was removed, and Cy3 labeled siGL3 (Cy3-siGL3) was purified by ethanol precipitation.

***In Vivo* Study** Six-week-old male ICR mice were used in this study. All mice were anesthetized intraperitoneally with pentobarbital (50 mg/kg). Their backs were shaved with an electric clipper and hair was removed with a cream-based hair remover (Kanebo, Tokyo, Japan). The backs of the mice were then tape-stripped 0—20 times by surgical tapes (Trans pore, U.S.A.) and each of the 25 μl of siRNA (FAMsiRNA or Cy3-siGL3) samples (naked siRNA, Tat/siRNA complex (Tat), siRNA and AT1002 mixing solution (AT1002), and Tat/siRNA complex and AT1002 mixing solution (Tat+AT1002)) were applied to the backs of the mice. After 10 h, the mice were sacrificed and their dermal tissues were washed with phosphate-buffered saline and resected in 1-cm^2 cross-sections of tissues containing the sample application site. The tissues were soaked in Tissue Mount (Shiraimatsu, Osaka, Japan) at 4 °C in the dark overnight and mounted with Tissue Mount in cold-acetone. The tissues were preserved at −40 °C. To exam-

ine skin permeability of the siRNAs in mice, 20 μm (x–y images) and 40 μm (z-series) frozen sections of skin were prepared by Cryostat HM550 and fixed in cold-acetone. The slides were washed with PBS solution three times and mounted with Fluoroment-G. FAMsiRNA in the skin was observed by confocal laser microscopy.

Statistical Analysis All values represent the mean±S.D. or S.E. Statistical analysis of the data was performed using a paired Student's t-test. Statistical significance was defined as $*p<0.05$ and $**p<0.01$.

Results

siRNA Stability against RNaseA with Tat and AT1002 and Characteristics of Tat/FAMsiRNA The stability of siRNA dissolved with Tat and AT1002 against RNaseA was assessed. Figure 1 shows the relative remaining siRNA labeled with SYBER®Green with or without functional peptides at the various mixing time with RNaseA. In the case of naked siRNA, fluorescence intensity of the labeled siRNA almost disappeared 15 min after adding RNaseA. In contrast, AT1002 and Tat peptides dissolved separately with the siRNA and clearly improved the stability of the siRNA against RNaseA. However, when AT1002 and Tat were used in combination, approximately 60% of the siRNA remained over 10 h after adding RNaseA. The mean diameter and zeta-potential of the Tat/FAMsiRNA complex was approximately 70 nm and +4 mV, respectively.

Silencing Effects of the Tat/siRelA Complex Figure 2 shows the silencing effects of RelA mRNA in PAM212 cells (mouse keratinocytes) transfected with siRelA complexed with Tat. As shown in Fig. 2, naked siRelA cannot silence the RelA mRNA due to its low cellular uptake ability. In contrast, by using Tat (N/P=10), the mRNA of RelA was silenced by siRelA. The silencing effects of Tat/siRelA (N/P=10) show a high value in the PAM212 cells. These results indicate that siRelA designed in this study can silence the mRNA of RelA and that Tat is a good carrier for siRelA delivery into cells related to atopic diseases.

Effect of AT1002 on ZO-1 Constitution in Mouse Skin The effect of AT1002 on the constitution of ZO-1 in mouse skin was examined. As shown in Fig. 3, in the control mouse (no treatment), fluorescence of immunostained-ZO-1 was clearly localized at the intercellular gap (Fig. 3a). In the mice with AT1002 applied to their skin, fluorescence of ZO-1 could hardly be detected 1 h after application and 10 h later; fluorescence of ZO-1 almost could not be observed at all (Fig. 3b). This phenomenon of decreased ZO-1 fluorescence is due to AT1002 inducing tight junction permeability by causing tyrosine phosphorylation of ZO-1.[30] Subsequently, recovery of fluorescence of ZO-1 was determined in the same way. Figure 3b shows that in the mouse skin applied with AT1002 for 10 h and then washed with PBS, ZO-1 re-localized over time. As a result, 7 h after washing the skin, recovery of ZO-1 localization was observed (Fig. 3c), yet still not completely, indicating that the effect of AT1002 on ZO-1 constitution in the skin might be reversible.

Transdermal siRNA Delivery by Using Tat and AT1002 Figure 4a shows the histological sections of mouse skin tape-stripped 0, 10 and 20 times on the back and stained with hematoxylin and eosin. The thickness of stratum corneum

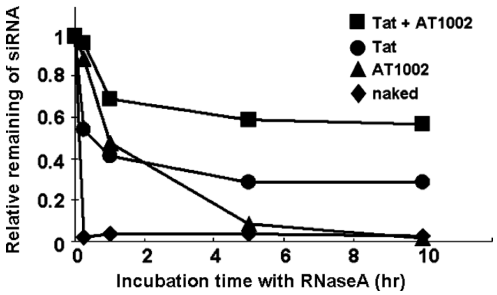

Fig. 1. Effect of Tat and AT1002 on siRelA Stability against RNaseA

RNaseA (10 μg) was added to naked siRelA (naked), Tat/siRelA (Tat), siRelA with AT1002 (AT1002), and Tat/siRelA with AT1002 (Tat+AT1002), and incubated at 37 °C for 0—10 h. The siRelA was decondensed from siRelA complexes by adding 0.01 mM dextran sulfate and then labeled with SYBER®Green. Relative remaining amount of siRelA was determined using a microplate reader. The data are expressed as the relative remaining siRNA ratio *versus* the siRNA fluorescence value at 0 h ($n=1$).

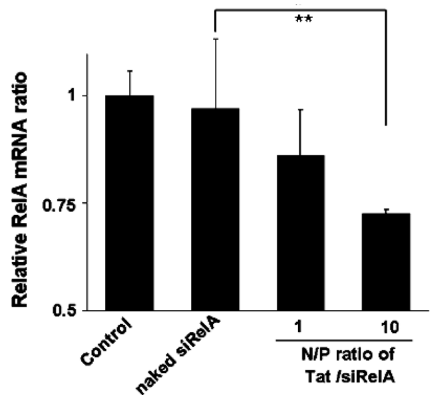

Fig. 2. RelA mRNA Expression in PAM212 Cells after Transfection with Either Naked siRelA or Tat/siRelA Complexes

The naked siRelA and Tat/siRelA complexes (N/P=1, 10) were transfected into PAM212 cells (siRelA 0.05 μg) for 24 h. After transfection, the cells were stimulated with LPS for 8 h. RelA mRNA was measured by RT-PCR. The relative RelA mRNA was calculated based on the RelA mRNA of the control group. Each bar represents the mean±S.D. ($n=4$). $**p<0.01$ (t-test).

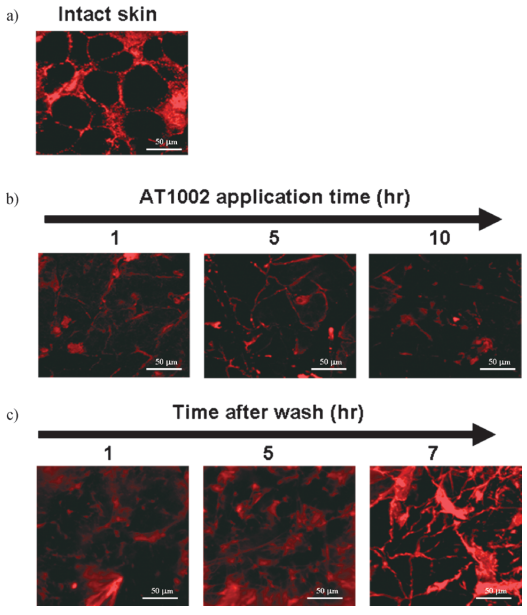

Fig. 3. Effect of AT1002 on ZO-1 Distribution in Mouse Skin

Skin sections were fixed and processed by immunofluorescence to detect ZO-1 distribution. The stained skin sections were observed using a confocal laser microscope at ×20 magnification. (a) Intact mouse back skin (b) AT1002 applied to mouse back skin for 1—10 h AT1002 (400 μg) was applied to 20 times tape-stripped back skin of ICR mice for 1, 5, and 10 h (c) recovery of ZO-1 distribution in AT1002-applied mouse back skin. AT1002 (400 μg) was applied to tape-stripped back skin of ICR mice. Ten hours later the AT1002 was removed, the skin was washed, and then harvested after a lapse of 1, 5, and 7 h.

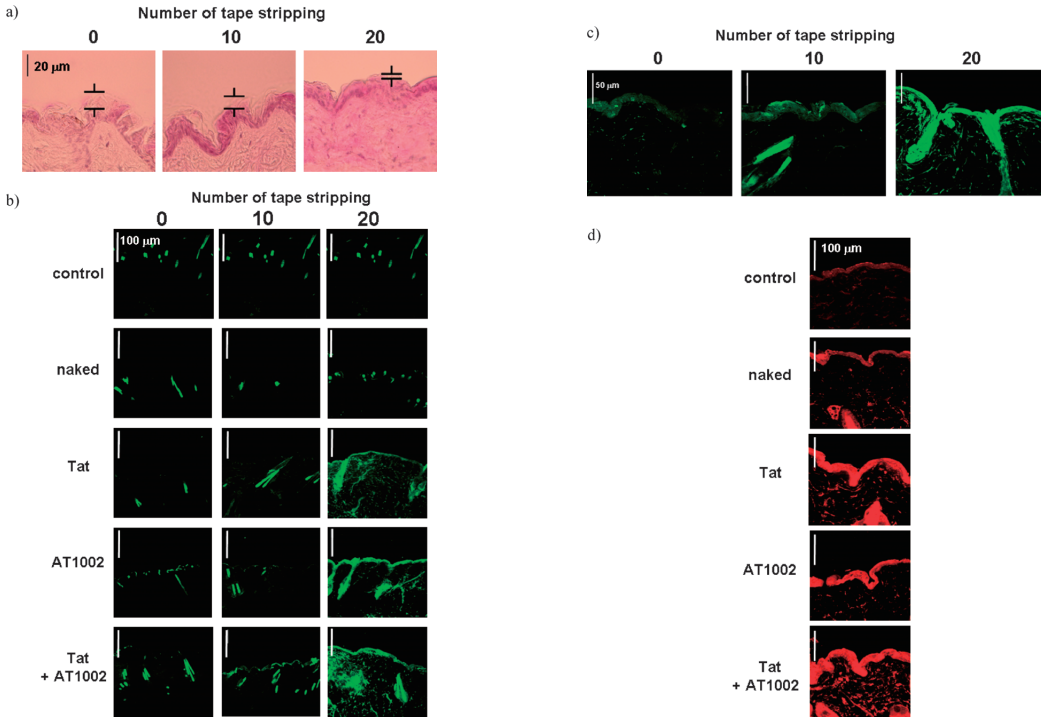

Fig. 4. (a) Effect of the Number of Tape Stripping Times on the Stratum Corneum

HE stained back skin sections of tape-stripped ICR mice were observed with an optical microscope (magnification: ×60).

(b—d) Permeability of (b, c) FAMsiRNA in 0, 10, and 20 Times Tape-Stripped Back Skin of ICR Mice or (d) Cy3-siGL3 in 20 Times Tape-Stripped Back Skin of ICR Mice

Naked siRNA (5 μg), Tat/siRNA (32 μg/5 μg), siRNA with AT1002 (5 μg+400 μg), and Tat/siRNA with AT1002 (32 μg/5 μg+400 μg) were applied to 0, 10, and 20 times tape-stripped back skin of ICR mice for 10 h. The frozen skin sections (20 μm) were observed using a confocal laser microscope. (magnification: (b); ×20, (c); ×60, (d); ×20.

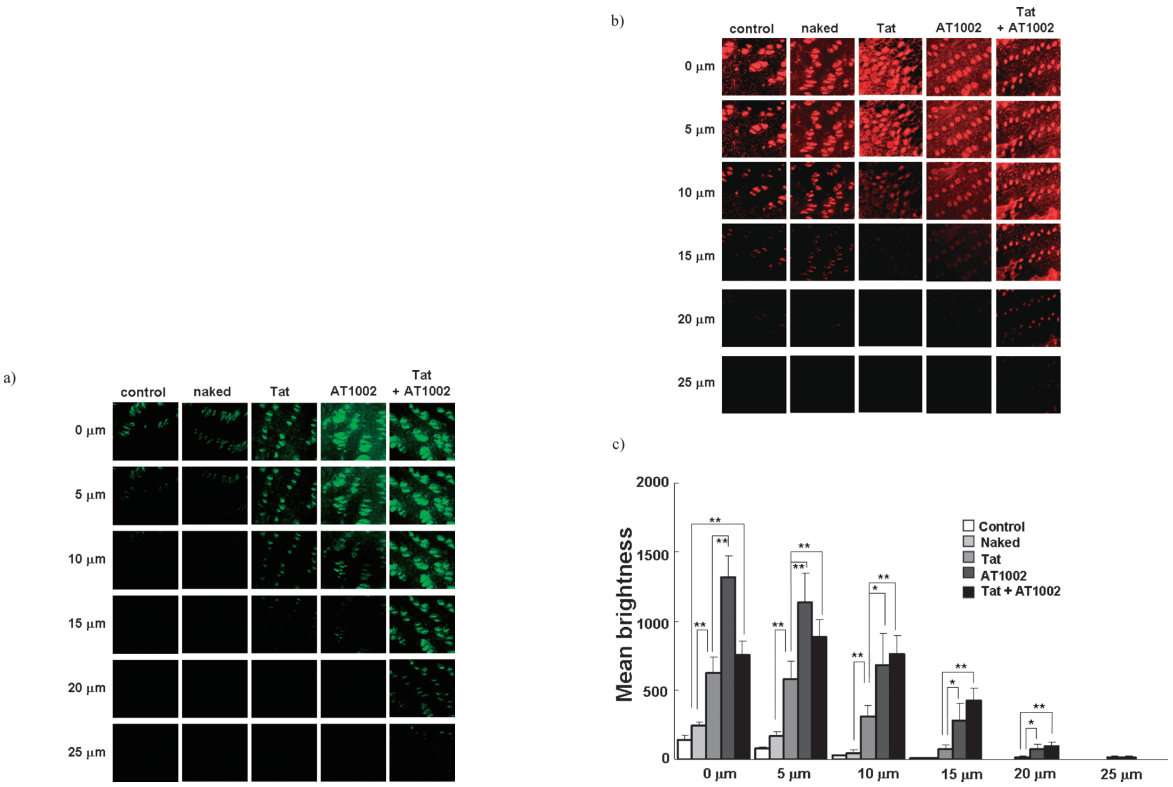

Fig. 5. (a) FAM-siRNA or (b) Cy3-siGL3 Localization in *x–z* after 20 Times Back Stripping the Skin of ICR Mice

Naked siRNA (5 μg, Naked), Tat/siRNA (32 μg/5 μg, Tat), siRNA with AT1002 (5 μg+400 μg, AT1002), and Tat/siRNA with AT1002 (32 μg/5 μg+400 μg, Tat+AT1002) were applied to 0, 10, and 20 times tape-stripped back skin of ICR mice for 10 h. The frozen skin sections (40 μm) were observed using a confocal laser microscope in a horizontal direction. (magnification: ×20).

(c) Brightness Distribution of Localized FAM-siRNA in *x–z* Sections of 20 Times Tape-Stripped Back Skin

Each bar represents the mean±S.E., ($n=5$). $*p<0.05$, $**p<0.01$ (*t*-test).

was decreased dependently with the number of times of tape stripping, and after 20 times of stripping, the stratum corneum was almost completely removed.

Next, naked siRNA (Naked), the Tat/siRNA complex (Tat), the AT1002 and siRNA solution (AT1002), or the Tat/siRNA complex and AT1002 solution (Tat+AT1002) were applied to the tape-stripped mouse skin for 10 h, and localization of the siRNAs (FAMsiRNA or Cy3-siGL3) in the frozen skin sections was observed by confocal laser scanning microscopy. As shown in Fig. 4b, the fluorescent signals of FAMsiRNA in the no tape-stripped and 10 times tape-stripped skin could not be observed in any region in the no treatment (control), Naked- and Tat-applied skin samples. In contrast, fluorescent signals of FAMsiRNA in the AT1002-applied skin were observed faintly at the stratum corneum. Furthermore, in the Tat+AT1002-applied skin, FAMsiRNA was observed strongly at the stratum corneum. On the other hand, in the experiment using 20 times tape-stripped skin applied with Tat or AT1002, the FAMsiRNA (Fig. 4b) and Cy3-siGL3 (Fig. 4d) was observed widely and strikingly at the stratum corneum, the hair follicle, and the epidermal and dermal layers. Furthermore, in Tat+AT1002 applied to 20 times tape-stripped skin, the FAMsiRNA and Cy3-siGL3 was observed stronger than that in the other skins.

Subsequently, the high-powered field of stratum corneum in the 0, 10 or 20 times tape-stripped back skin applied with Tat and AT1002 showed FAMsiRNA fluorescence. As seen Fig. 4c, in no tape stripping and 10 times tape-stripped mouse skin, FAMsiRNA fluorescence was mainly observed at the stratum corneum. Conversely, in stratum corneum-removed skin, strong fluorescence of FAMsiRNA was drastically observed at the stratum corneum and also the hair follicle, and epidermal and dermal layers.

In Figs. 5a and b horizontal sections of 20 times tape-stripped mouse skin applied with naked siRNA (Naked), Tat/siRNA (Tat), siRNA with AT1002 (AT1002), or Tat/siRNA with AT1002 (Tat+AT1002) are shown. We utilized two kinds of siRNA (FAMsiRNA and Cy3-GL3) to confirm the repeatability of this study. The photographs represent sliced images of mouse skin from the surface and up to 30-μm depth. In the control and naked siRNA-applied mouse skin, only intrinsic fluorescence of hair was observed. On the other hand, in the Tat- and AT1002-applied skin, siRNA was observed more deeply. When using the AT1002 peptide, siRNA was localized throughout the whole region of the surface of the skin, whereas with Tat, almost all of the siRNA was localized at the hair follicle. When Tat+AT1002 was applied to the skin, siRNA was localized more widely and deeply, thus indicating that the combination of Tat and AT1002 peptides was useful for transdermal siRNA delivery.

Figure 5c shows the numerical analysis of the brightness of localized FAMsiRNA in horizontal sections of 20 times tape-stripped mouse back skin after transdermal application of FAMsiRNA with or without the functional peptides. When using the Tat peptide, even though the brightness was higher than that with naked FAMsiRNA, the brightness was clearly decreased at 10-μm depth. However, when using the AT1002 peptide, the brightness could still be observed to up to 20-μm in depth. Finally, when combining both the AT1002 and Tat peptides the brightness of the FAMsiRNA in the stratum corneum was much stronger and deeper than that with AT1002 alone.

Discussion

Topical use of siRNA as a therapeutic nucleic acid has been increasingly studied for its applicability in treating skin diseases. However, transdermal naked siRNA delivery is limited due to its low stability in the skin and low permeability by various skin barriers such as the stratum corneum (multiple lipid bilayers) and epidermal layer (intercellular connection by tight junctions). In this study, we investigated whether the modulator peptide of tight junctions AT1002 and the cell penetrating peptide Tat could be used to easily and effectively deliver siRNA transdermally to the skin for the treatment of various skin diseases.

As our targeted disease in this study was atopic dermatitis (AD) in which the stratum corneum was disrupted, we used tape-stripping methods to disrupt the skin surface to mimic an AD-like skin model in our mice. Although the cells of the stratum corneum are broken and peeled off in AD disease, tight junction barriers still exist at the granular layer in the epidermal tissue. Therefore, our aim was to develop an effective transepidermal siRNA delivery system through both the paracellular and transcellular routes by using AT1002, which has tight junction opening ability, and Tat, which has siRNA condensation ability and intracellular penetration.

Firstly, the silencing effect on RelA mRNA in PAM212 cells transfected with siRelA complexed with Tat was markedly stronger than that with siRNA only, indicating that siRelA complexed with Tat can penetrate into the cells and silence RelA mRNA in skin cells. The effects of AT1002 on ZO-1 (an important tight junction protein) in the skin were examined. As shown in Fig. 3, ZO-1 on the surface of the epidermis was hardly observed in AT1002-applied skin, yet a tendency toward recovery around 7 h after washing was observed, thus demonstrating that this modulating effect was reversible. Furthermore, a previous report shows that in a mucosal absorption experiment AT1002 assists in tight junction opening for drug delivery and has reversible tight junction modulation.[30] These findings suggest that AT1002 can also act on skin as a tight junction modulator by opening tight junctions and facilitating transdermal drug delivery. As shown in Table 3, the Tat/FAMsiRNA complex is approximately 70 nm and +4 mV. In general, the size of paracellular routes in the epidermis and hair follicles is reported to be about 70 nm and 200 nm, respectively. Therefore, we assumed that the 70 nm Tat/FAMsiRNA nanocomplex could easily penetrate paracellularly the tight junctions of the disrupted epidermis from either the skin surface or hair follicle routes. Actually, in the intact epidermis, the Tat/FAMsiRNA complex was mainly observed in the hair follicles (Fig. 4b), not the whole epidermis. By contrast, in the case of AT1002 alone, FAMsiRNA was localized throughout the surface of the skin but not at deep sites. This result is most likely attrib-

Table 3. Mean Diameter and Zeta-Potential of the Tat/FAMsiRNA (N/P=10) Complex

Mean diameter (nm)	Zeta-potential (mV)
72.4±8.33	4.12±0.84

mean±S.D., n=3.

uted to the low stability and cellular permeability of the siRNA with AT1002 (Fig. 1). In both the surface and at deep sites, we believe that AT1002 acts as a tight junction modulator. However, the siRNA was degraded at the deep sites. On the other hand, when Tat and AT1002 were used in combination the stability of the siRNA against RNaseA clearly improved. Therefore, in the case of combined Tat and AT1002, siRNA was observed not only in hair follicles but also throughout the epidermis and dermis widely (Figs. 4, 5). This indicates that the tight junction modulator, AT1002, increases the permeation of siRNA at the epidermis due to its ability to modulate tight junction proteins, and that the efficacy of the siRNA delivery was enhanced by the siRNA-stabilizing and cell penetrating properties of the Tat peptide.

In summary, our novel transdermal siRNA delivery system using peptides with tight junction modulating and cell penetrating properties is easy to perform and does not require the use of instruments such as that required with electroporation, iontophoresis and sonophoresis. Furthermore, this system of skin damage by tight junction disruption is not too serious because the effect is reversible. Therefore, the siRNA topical application system reported here has therapeutic potential for the treatment of incurable skin diseases such as atopic dermatitis.

Acknowledgements We thank Ms. Misako Kawai, Ms. Yuuko Igarashi and Ms. Mayu Takeuchi (School of Pharmacy, Tokyo University of Pharmacy and Life Sciences) for their excellent technical assistance. We are also grateful to Prof. Tsunehiko Fukuda, Ph. D. (Nagahama Institute of Bio-Science and Technology) for peptide synthesis. This study was supported in part by Grant-in-Aid for Young Scientists (B) (60434015) from the Japan Society for the Promotion of Science and in part by a Grant for private universities provided by the Promotion and Mutual Aid Corporation for Private Schools of Japan.

References

1) Partidos C. D., Beignon A. S., Mawas F., Belliard G., Briand J. P., Muller S., *Vaccine*, **21**, 776—780 (2003).
2) Lopes L. B., Brophy C. M., Furnich E., Flynn C. R., Sparks O., Komalavilas P., Joshi L., Panitch A., Bentley M. V., *Pharm. Res.*, **22**, 750—757 (2005).
3) Proksch E., Brandner J. M., Jensen J. M., *Exp. Dermatol.*, **17**, 1063—1072 (2008).
4) Brandner J. M., Kief S., Wladykowski E., Houdek P., Moll I., *Skin Pharmacol. Physiol.*, **2006**, 1971—1977 (2006).
5) Brandner J. M., Proksh E., "Skin Barrier," ed. by Ellas P. M., Feingold K. R., Taylor and Francis, New York, 2006, pp. 191—210.
6) Ohnemus U., Kohmeyer K., Houdek P., Rohde H., Wladykowski E., Vidalet S., Horstkotte M. A., Aepfelbacher M., Kirschner N., Behne M. J., Moll I., Brandner J. M., *J. Invest. Dermatol.*, **128**, 906—916 (2008).
7) Ranaldi G., Marigliano I., Vespignani I., Perozzi G., Sambuy Y., *J. Nutr. Biochem.*, **13**, 157—167 (2002).
8) Valenta C., Auner B. G., *Eur. J. Pharm. Biopharm.*, **58**, 279—289 (2004).
9) Thanou M., Verhoef J. C., Junginger H. E., *Adv. Drug Deliv. Rev.*, **52**, 117—126 (2001).
10) Sonoda N., Furuse M., Sasaki H., Yonehara S., Katahira J., Horiguchi Y., Tsukita S., *J. Cell. Biol.*, **147**, 195—204 (1999).
11) Takahashi A., Kondoh M., Masuyama A., Fujii M., Mizuguchi H., Horiguchi Y., Watanabe Y., *J. Cell. Biol.*, **108**, 56—62 (2005).
12) Kondoh M., Masuyama A., Takahashi A., Asano N., Mizuguchi H., Koizumi N., Fujii M., Hayakawa T., Horiguchi Y., Watanabe Y., *Mol. Pharmacol.*, **67**, 749—756 (2005).
13) Fasano A., Fiorentini C., Donelli G., Uzzau S., Kaper J. B., Margretten K., Ding X., Guandalini S., Comstock L., Goldblum S. E., *J. Clin. Invest.*, **96**, 710—720 (1995).
14) Fasano A., Uzzau S., *J. Clin. Invest.*, **99**, 1158—1164 (1997).
15) Watts T., Berti I., Sapone A., Gerarduzzi T., Not T., Zielke R., Fasano A., *Proc. Nat. Acad. Sci. U.S.A.*, **102** 2916—2921 (2005).
16) Song K. H., Fasano A., Eddington N. D., *Int. J. Pharm.*, **351**, 8—14 (2008).
17) Song K. H., Fasano A., Eddington N. D., *Eur. J. Pharm. Biopharm.*, **69**, 231—237 (2008).
18) Synder E. L., Dowdy S. F., *Expert Opin. Drug Deliv.*, **2**, 43—51 (2005).
19) Chang M., Chou J. C., Lee H. J., *Plant Cell Physiol.*, **46**, 482—488 (2005).
20) Wadia J. S., Dowdy S. F., *Curr. Opin. Biotechnol.*, **13**, 52—56 (2002).
21) Dietz G. P., Bahr M., Mol. *Cell Neurosci.*, **27**, 85—131 (2004).
22) Kim D., Jeon C., Kim J. H., Kim M. S., Yoon C. H., Choi I. S., Kim S. H., Bae Y. S., *Exp. Cell Res.*, **312**, 1277—1288 (2006).
23) Shokolenko I. N., Alexeyev M. F., LeDoux S. P., Wilson G. L., *DNA Repair*, **4**, 511—518 (2005).
24) Melikov K., Chernomordik L. V., *Cell Mol. Life Sci.*, **62**, 2739—2749 (2005).
25) Rothbard J. B., Garlington S., Lin Q., Kirschberg T., Kreider E., McGrane P. L., Wender P. A., Khavari P. A., *Nat. Med.*, **6**, 1253—1257 (2000).
26) Robbins P. B., Oliver S. F., Sheu S. M., Goodnough J. B., Wender P., Khavari P. A., *BioTechniques*, **33**, 190—194 (2002).
27) Hou Y. W., Chan M. H., Hsu H. R., Liu B. R., Chen C. P., Chen H. H., Lee H. J., *Exp. Dermatol.*, **16**, 999—1006 (2007).
28) Kanazawa T., Takashima Y., Hirayama S., Okada H., *Int. J. Pharm.*, **360**, 164—170 (2008).
29) Tanaka K., Kanazawa T., Shibata Y., Suda Y., Fukuda T., Okada H., *Int. J. Pharm.*, **396**, 229—238 (2010).
30) Gopalakrishnan S., Pandy N., Tamiz A. P., Vere J., Carrasco R., Somervile R., Tripathi A., Ginski M., Paterson B. M., Alkan S. S., *Int. J. Pharm.*, **365**, 121—130 (2009).